# HyLogger Case Study: Greenbushes (C3DD024)

## Pt. 1 Geological Context and Introduction to NVCL Datasets

Stromberg, J., Laukamp, C., Hancock, L., Wawryk, M., Duuring, P., LeGras, M.

National Virtual Core Library (NVCL) Project

Geological Survey of Western Australia

# Summary

This case study includes a HyLogger data pack for drill hole C3DD024 (Greenbushes Li-Sn-Ta pegmatite deposit, Western Australia) comprising hyperspectral drill core reflectance spectra ("HyLogger data"), geochemistry, and lithology data, as well as a case study report split into several parts. The *.tdg file* allows full access to the data and CSIRO's The Spectral Geologist software (TSG™) without a full TSG software license required for this dataset. Part I of the case study report outlines the geological context of the C3DD024 drill hole, providing the necessary background for interrogating the datasets. It will also provide an overview of the datasets available with the case study. Subsequent parts of the case study will aim to interrogate specific geological questions using this dataset, such as white mica and smectite alteration signatures. New applications-based sections will be added periodically to the case study and will use the same datasets.

# Geological Context

The Greenbushes Li-Sn-Ta pegmatite deposit is a world class Li mineral asset and occurs ~350 km south of Perth, in Western Australia, in the Southwest Terrane Greenstones of the Yilgarn Craton (Figure 1). The Greenbushes deposit presently supplies more than 30% of the worlds lithium and is the single largest Li hard rock deposit in the world. Development of the Greenbushes Li orebody began in 1983, however, the Greenbushes areas has been mined for tin since 1888 and tantalum since 1984 (Talison Lithium). The resource for Greenbushes was 158.06 Mt of ore at a grade of 2.25 wt% $Li_2O$ for 8.72 Mt of lithium carbonate equivalent in 2015 and has been continuously mined since this time (Partington, 2017).

The Greenbushes pegmatites are rare-element pegmatites belonging to the Lithium-Caesium-Tantalum (LCT) family and occurs in the Archean Western Gneiss Terrane (Figure 1). The pegmatites intruded into the Balingup Metamorphic Belt along the 2.53 Ga Donnybrook-Bridgetown shear zone. This shear zone is NNW trending, 15-20 km wide, and consists of sheared gneisses, amphibolite, and syn-tectonic granitic intrusions (Partington et al, 1995).

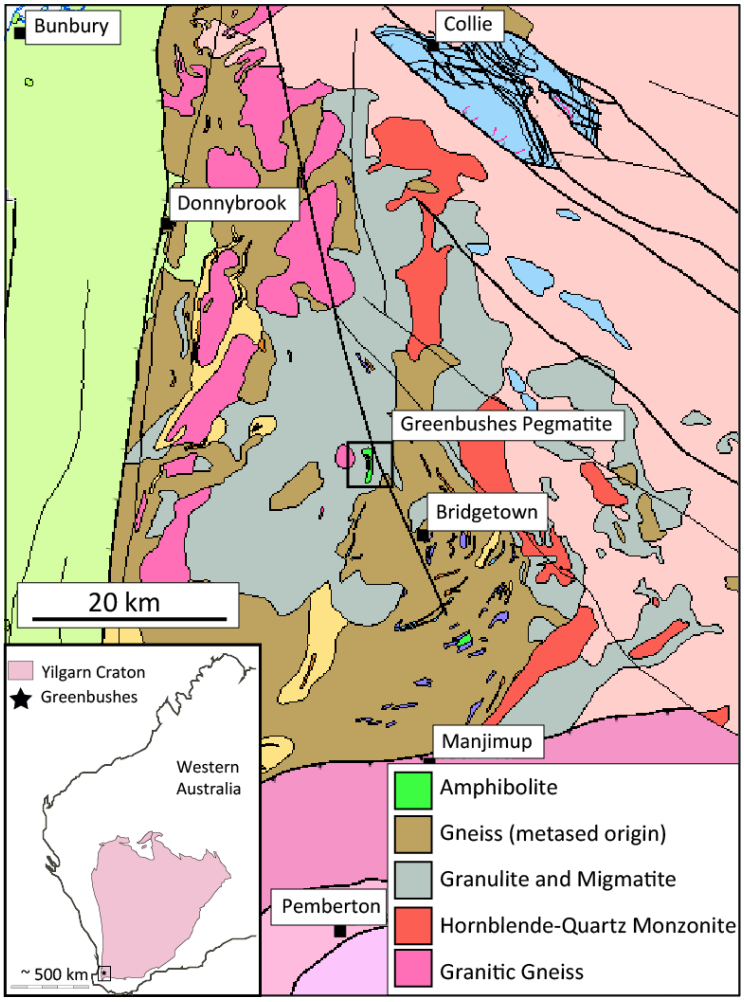


**Figure 1 Regional map showing the geology and location of the Greenbushes Pegmatite in the southwest corner of the Yilgarn craton (modified after Duuring, 2020 and GeoVIEW.WA, 2016)**

The region has undergone several stages of deformation beginning with the formation of the Bridgetown gneisses at 3.1 Ga, deformation and intrusion of regional granites from 2.61 to 2.58 Ga, followed by intrusion and deformation of the Greenbushes Pegmatite at 2.53 Ga (Partington et al, 1995). The pegmatites were intruded by dolerite dykes at 2.43 Ga resulting in some hydrothermal remobilization followed by several younger deformation and intrusion events. For a detailed summary of the regional deformation history, see Partington et al, 1990, 1995 and Partington, 2017. The mineralization at the Greenbushes Pegmatite is unusual in that it occurs in a high-temperature and high-pressure metamorphic terrane but was intruded 50 Ma after regional granite intrusion and so is not associated with any known proximal fractionated granites (Partington, 2017).

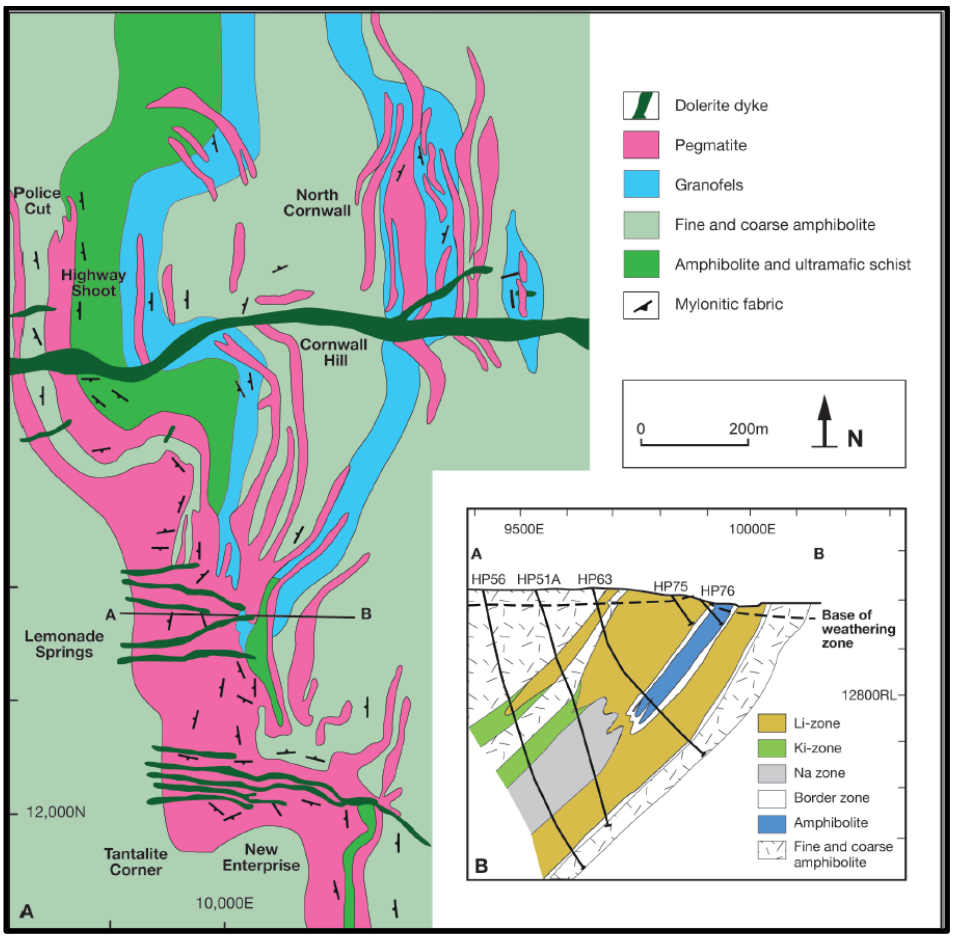


**Figure 2 Mine scale geology of the Greenbushes with an inset cross section (A-B) showing the pegmatite zonation and distribution of Lithium in the main ore zone (From Partington, 2017)**

The pegmatites occur within shear zones at the contact between major sequences of country rock (granofels, ultramafic schist, amphibolite) and are crosscut by dolerite dykes. The pegmatites are mineralogically zoned and consist of a series of linear intrusions which are 2-3 km in strike and 10 to 300 m thick (Figure 2). The main Li zone is over 2 km long and the main ore mineral is spodumene, a Li-pyroxene ($LiAl(SiO_3)_2$), which is mined in open pits from fresh, unweathered zones of pegmatite and often accounts for up to 50% of the rock volume (Partington, 2017). The mineral zonation observed in the Greenbushes pegmatites is unusual with the most Li-rich zones occurring in the hanging wall and footwall zones, surrounding the albite zone. In general, the albite zone hosts the highest-grade tin and tantalum ore shoots (Figure 2, Partington, 2017).

# Drill Hole Context

Drill hole C3DD024 was drilled from within the Central Lode open pit and collared in fresh pegmatite (Table 1). It encounters over 200 m of pegmatite in the main lithium ore zone and was drilled to better constrain boundaries of the pegmatite resource (Hancock and Wawryk, 2020). The drill hole also intersects minor (<1 m wide) dolerite units and finishes in ~10 m of amphibolite (Table 2; Figure 3; Figure 4).

Table 1 Drill hole details (Hancock and Wawryk, 2020)

| Hole | Lat (°E) | Long (°s) | Elevation | Inclination (°)[5] | Azimuth (TN)[6] | EOH |
|---|---|---|---|---|---|---|
| C3DD024 | 116.0651289 | -33.85920461 | 205.186 | -59.7 | 077.2 | 246.5 m |

Table 2 Summary of the geology log for C3DD024 (Hancock and Wawryk, 2020)

| From | To | Lithology |
|---|---|---|
| 0 | 153.63 | Pegmatite |
| 153.63 | 154.41 | Dolerite |
| 154.41 | 156.07 | Pegmatite |
| 156.07 | 159.92 | Dolerite |
| 159.92 | 182.63 | Pegmatite |
| 182.63 | 182.82 | Dolerite |
| 182.82 | 196.19 | Pegmatite |
| 196.19 | 197.49 | Dolerite |
| 197.49 | 201.28 | Pegmatite |
| 201.28 | 201.61 | Dolerite |
| 201.61 | 218.79 | Pegmatite |
| 218.79 | 218.91 | Dolerite |
| 218.81 | 237.77 | Pegmatite |
| 237.77 | 246.5 | Amphibolite |

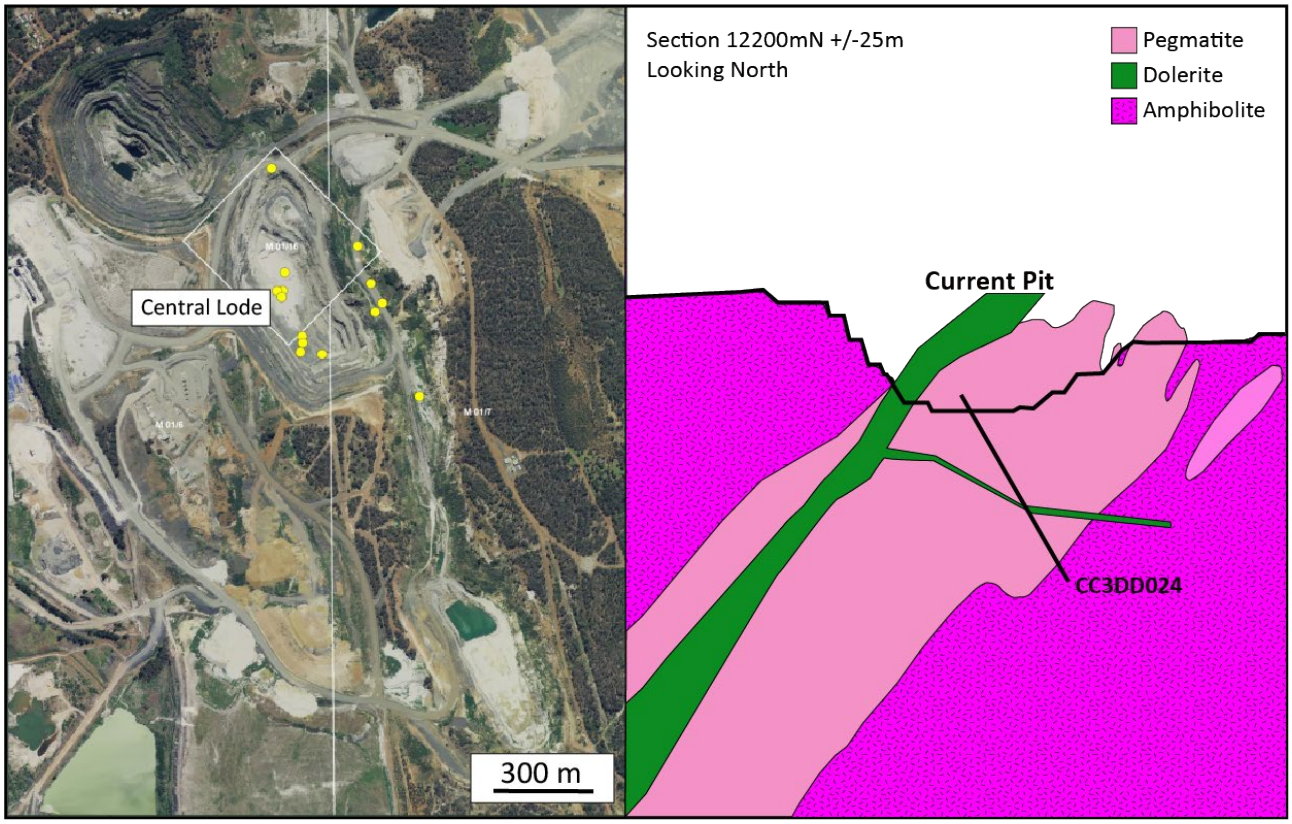


**Figure 3 Arial photo of the Greenbushes mine with 2014 drill collars marked as yellow circles and cross section of the Central Lode showing the position of drill hole CC3DD024 (modified from GSWA WAMEX Report A104943 and Talisan Lithium Pty Ltd)**

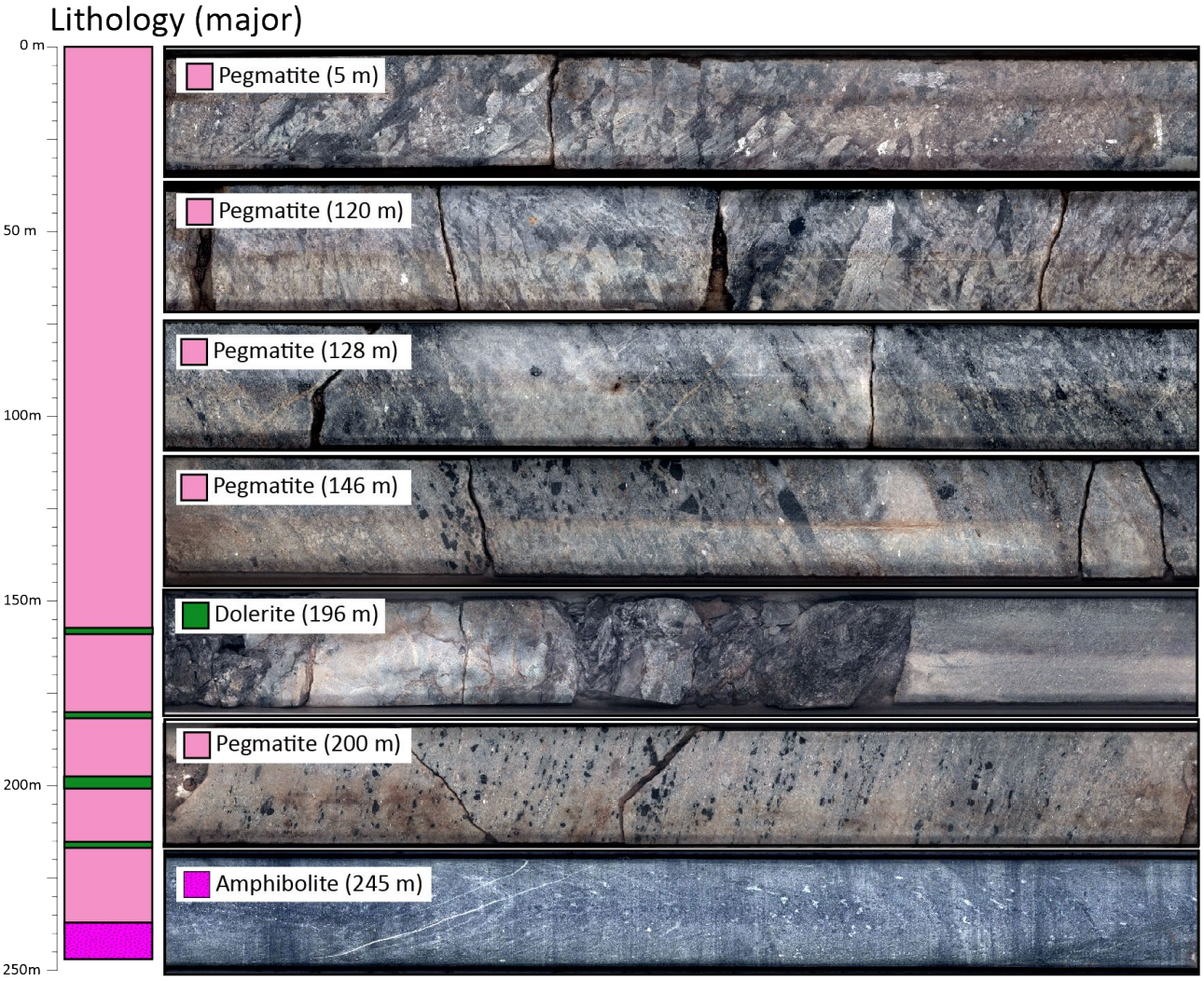


**Figure 4 Summary of the lithologies intersected in drill hole C3DD024 with HyLogger photos showing the variability in the pegmatite down hole from coarse grained spodumene at the top with to less spodumene rich to more feldspar rich with notable tourmaline towards the bottom.**

# Introduction to the Case Study Datasets

The TSG™ file in this case study dataset is provided as a *.tdg file* and includes HyLogger data (i.e. reflectance spectra, high-resolution RGB imagery, laser line profilometry) as well as some imported geochemistry and lithology information (visual logging). To view the HyLogger data, open the file ending in *.tdg* in TSG™.

This TSG™ file was generated by the HyLogger-3 system during analysis of the core at the Geological Survey of Western Australia (GSWA) using the method described by Hancock and Huntington (2010), Hancock et al. (2013) and Schodlok et al. (2016). Reflectance spectra were collected over the visible-to-near-infrared (VNIR 380– 1000 nm), short-wave infrared (SWIR 1000–2500 nm) and thermal infrared (TIR 6000– 14 500 nm) wavelength ranges and high-resolution (0.1 mm pixel) digital colour photographs of core were obtained concurrently using a built-in line-scan camera. The reflectance spectra were automatically resampled to 8 nm spectral sampling and 8 mm spatial resolution using TSG™.

The results discussed Part I of this case study are primarily based on The Spectral Assistant algorithm (TSA; Berman et al., 2017) outputs which are derived in the TSG™ software (e.g. Figure 4). TSA is an algorithm for automated spectral unmixing which uses a training spectral library to match the spectrum against a single mineral or model a simulated mixture of 2-4 minerals that most closely resembles that of the input spectrum (Berman et al., 2017). TSA mineralogy outputs are one of the most common outputs derived from hyperspectral data using TSG™ and for this dataset has been derived using expert input and domain knowledge. The SWIR and TIR spectral ranges are sensitive and diagnostic for different mineral groups, and so the SWIR and TIR TSA result are complementary and should be considered together (Figure 5).

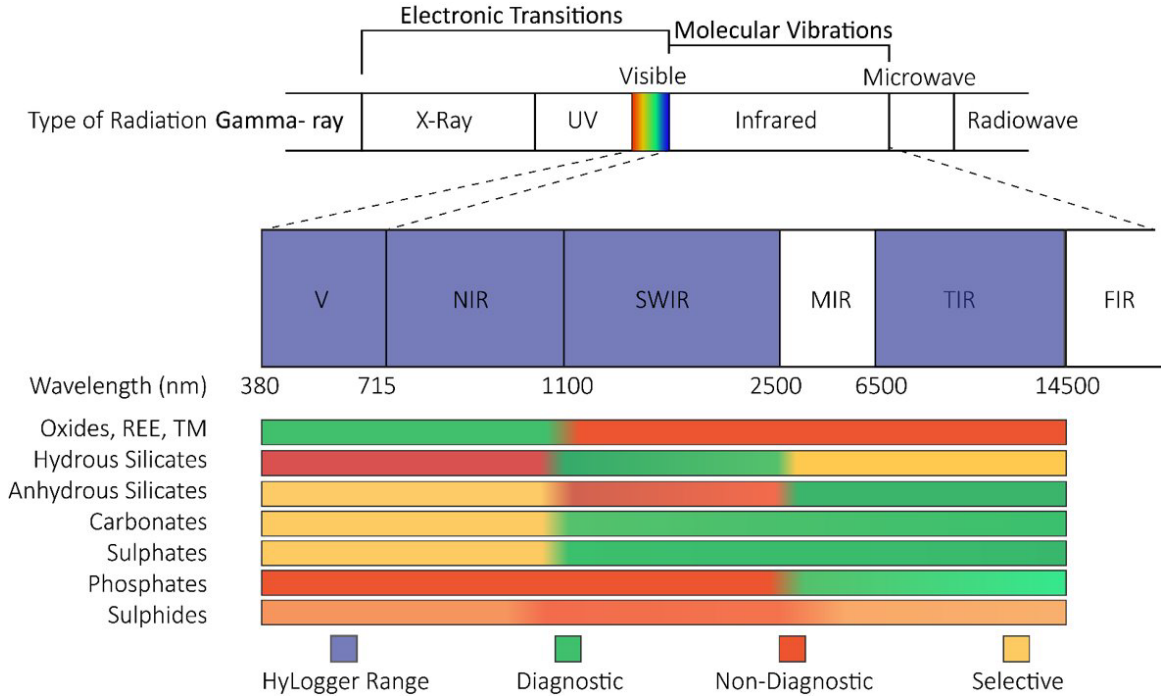


**Figure 5 Summary of the Hylogger spectra range and the mineral groups for which the VNIR, SWIR, and TIR are diagnostic, non-diagnostic, and selective.**

There are also several scalars discussed in the later parts of this case study (e.g, 2200D). Scalar is the term used by TSG™ to refer to any set of calculated values related to loaded spectral data. The scalars applied are pre-written, well-established, and in most cases published scripts for spectral parameters which probe the position or depth of a given spectral absorption feature. Batch system scalars commonly use a 3-band polynomial fit, while the User Scalars employ a Multiple Feature Extraction Method (Laukamp et al., 2010) for their outputs so are much more restrictive. Details of the scalars name, application, as well as references are included the explanatory notes of the report and in Laukamp et al., 2021.

The TSG™ file also includes some of the geochemistry data compiled by GSWA (Appendix "Assay_C3DD024_dmirs.csv"), which can be found under the scalars as imported numeric logs and are displayed in plot layout "XRF geochem log". A suite of 37 elements ($Al_20_3$, $As_2O_3$, BaO, $Bi_2O_3$, CaO, $CeO_2$, CoO, $Cr_2O_3$, $Cs_2O$, CuO, $Fe_2O_3$, $HfO_2$, $K_2O$, $La_2O_3$, $Li_2O$, MgO, MnO, $Na_2O$, $Nb_2O_5$, NiO, $P_2O_5$, PbO, $Rb_2O$, $Sb_2O_3$, $SiO_2$, $SnO_2$, $SO_3$, SrO, $Ta_2O_5$, $ThO_2$, $TiO_2$, $U_3O_8$, $V_2O_5$, $WO_3$, $Y_2O_3$, ZnO, $ZrO_2$) was obtained by GSWA from ~1m intervals of half drill core by means of XRF in 2015.

The lithology data (Appendix "Geology_C3DD024_dmirs2.csv") is captured as class scalars and are displayed in plot layout "lithology log".

# Downhole Summary

The most basic hyperspectral output from HyLogger datasets is the downhole mineralogy summary. This is displayed on the summary screen in TSG™ and provides an overview of the downhole hyperspectral mineralogy as derived from the TSA algorithm and can be binned at different sizes. Figure 6 shows the TSA derived downhole mineralogy for C3DD024, the major lithologies and whole rock geochemistry assays $Li_2O$, $K_2O$, $Na_2O$ and $Sn_2O$.

The TSA outputs in Figure 6 are split into SWIR and TIR mineralogy and represent spatial plots of the User SWIR and User jCLST results binned at the 1 m scale. Using only this summary plot, the major lithologies and contacts can be distinguished based on changes in the downhole spectral mineralogy. For instance, the contact between the pegmatite and footwall amphibolite is clearly identifiable by a marked increase in the proportion of amphibole group minerals in the bottom ~10 meters. The crosscutting dolerites are also easily distinguished by amphibole rich sections in the drill core.

It is also clear that while the drill hole intersects over 200 meters of pegmatite, that there are two mineralogical zones which are intersected in the pegmatite based on the thermal-infrared TSA results. The top 120 m of the drill hole contains pyroxene and a strong quartz signature, and the bottom 120 m is characterized by an abundance of K-feldspar, plagioclase and less quartz. This change in pegmatite mineralogy is more subtle in the SWIR results where SWIR TSA results are potentially dominated by smectite in the top 120 m with a notable tourmaline signature below that. However, this does not mean that the bulk mineralogy of the core is dominated by smectites. It is important to consider both the SWIR and TIR together, and which minerals are active in each spectral range when drawing conclusions from hyperspectral mineralogy. Part II of this case study will investigate the smectite and white mica SWIR signature further, in order to determine which di-octahedral sheet silicates are actually present in the respective drill core intervals.

The change in pegmatite mineralogy can also be observed in the core photography (Figure 4) and is also reflected in the downhole geochemistry (Figure 6). The top 120 m comprises the highest $Li_2O$ assay values which reflects the presence of spodumene (Li-pyroxene). The abundance of K-feldspar and plagioclase group minerals (albite) below that spodumene-quartz domain corresponds to higher $Na_2O$ and $K_2O$ values with respect to the top 120 m (Figure 6). This lower Feldspar-plagioclase-tourmaline domain is also characterized by higher $SnO_2$ values.

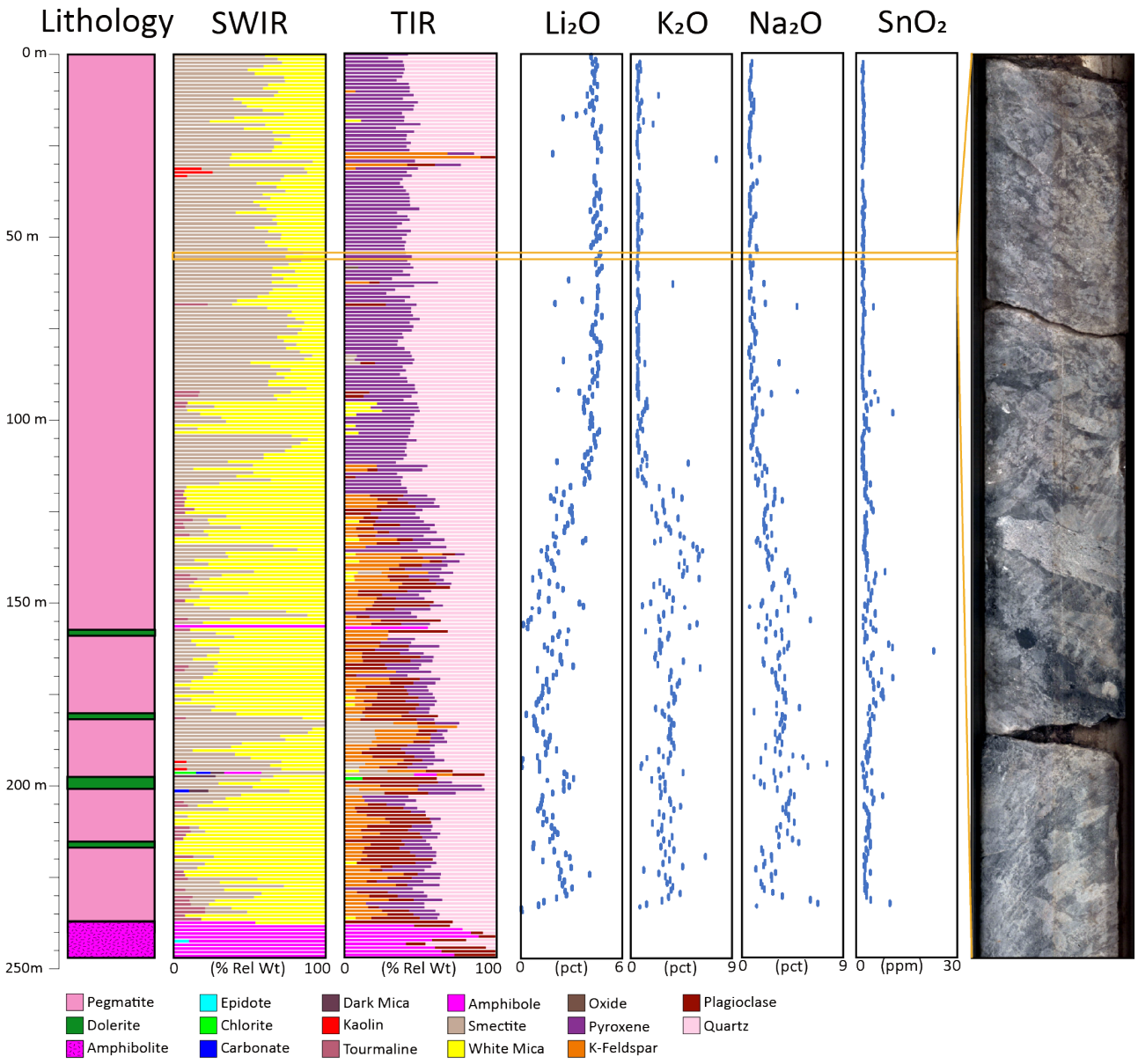


**Figure 6 Summary of the major lithologies, TSA-derived hyperspectral mineralogy by mineral group (after Hancock and Wawryk, 2020), and selected goechemical assays for C3DD024, as well as a core photo of a spodumene rich section**

# Saved plot layouts

A range of plot layouts are saved in the .tdg-file to help navigate the hyperspectral and geochemical data. The plot layouts in TSG can be accessed by selecting “View” > “Plot layouts”. For scripts applied in the plot layouts see Laukamp et al. (2021). For details about applying PLS-modelling of geochemical parameters to hyperspectral data see Laukamp et al. (2020).

## 1.1 Plot layout “log mineralmatch”

This plot layout features from left to right the depth (1st column), user-based TSA SWIR results of the first three mineral groups identified in the SWIR (columns 2, 3 and 4) and the related error (column 5), system-based jCLS TIR results of the first three mineral groups identified in the TIR (columns 6, 7, 8) and the related error (column 9), and the high-resolution linescan RGB imagery (column 10).

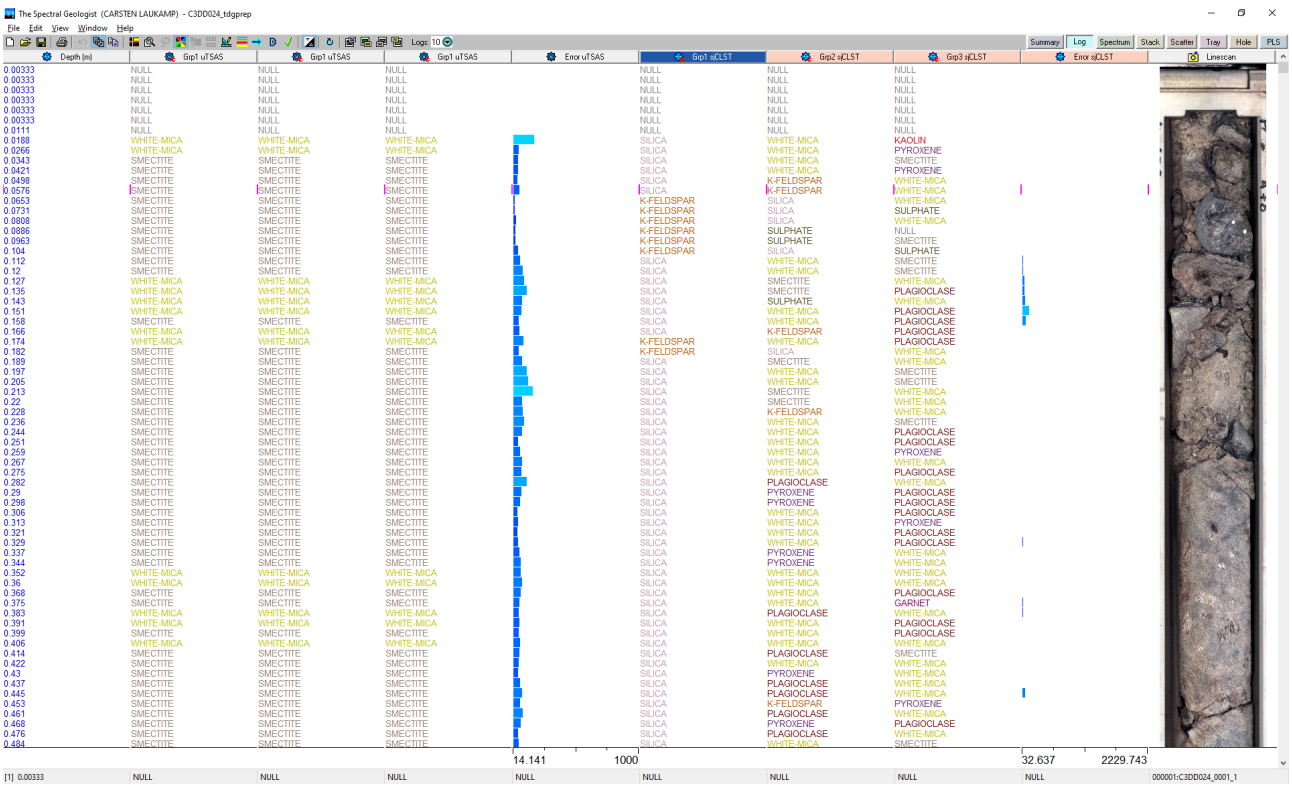

Figure 7 Plot layout “log mineralmatch”

## 1.2 Plot layout “log XRF geochem”

This plot layout features from left to right the whole rock XRF geochemistry results provided by GSWA ($Al_2O_3$, $As_2O_3$, BaO, $Bi_2O_3$, CaO, $CeO_2$, CoO, $Cr_2O_3$, $Cs_2O$, CuO, $Fe_2O_3$, $HfO_2$, $K_2O$, $La_2O_3$, $Li_2O$, MgO, MnO, $Na_2O$, $Nb_2O_5$, NiO, $P_2O_5$, PbO, $Rb_2O$, $Sb_2O_3$, $SiO_2$, $SnO_2$, $SO_3$, SrO, $Ta_2O_5$, $ThO_2$, $TiO_2$, $U_3O_8$, $V_2O_5$, $WO_3$, $Y_2O_3$, ZnO, $ZrO_2$).

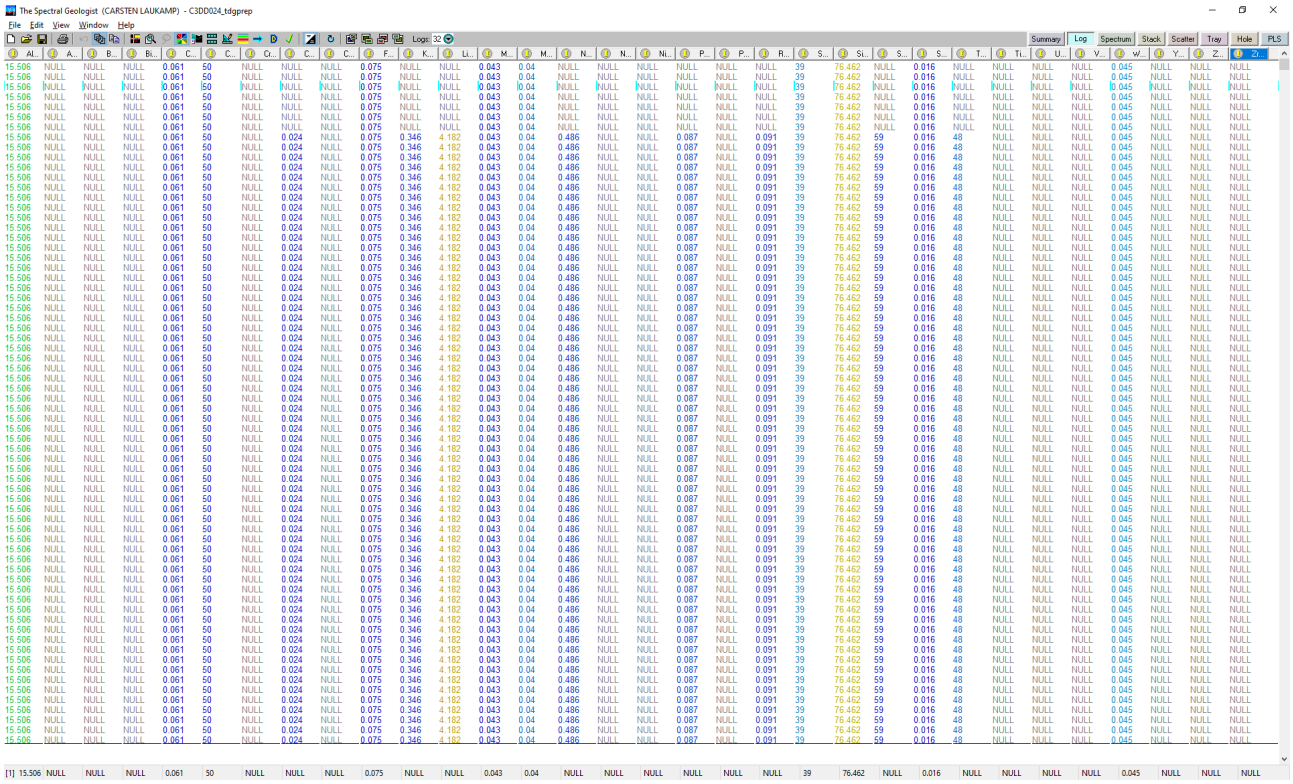

Figure 8 Plot layout “log XRF geochem”

## 1.3 Plot layout “lithology”

This plot layout features from left to right the depth (1st column), lithological code (2nd column) and the high-resolution linescan RGB imagery (3rd column).

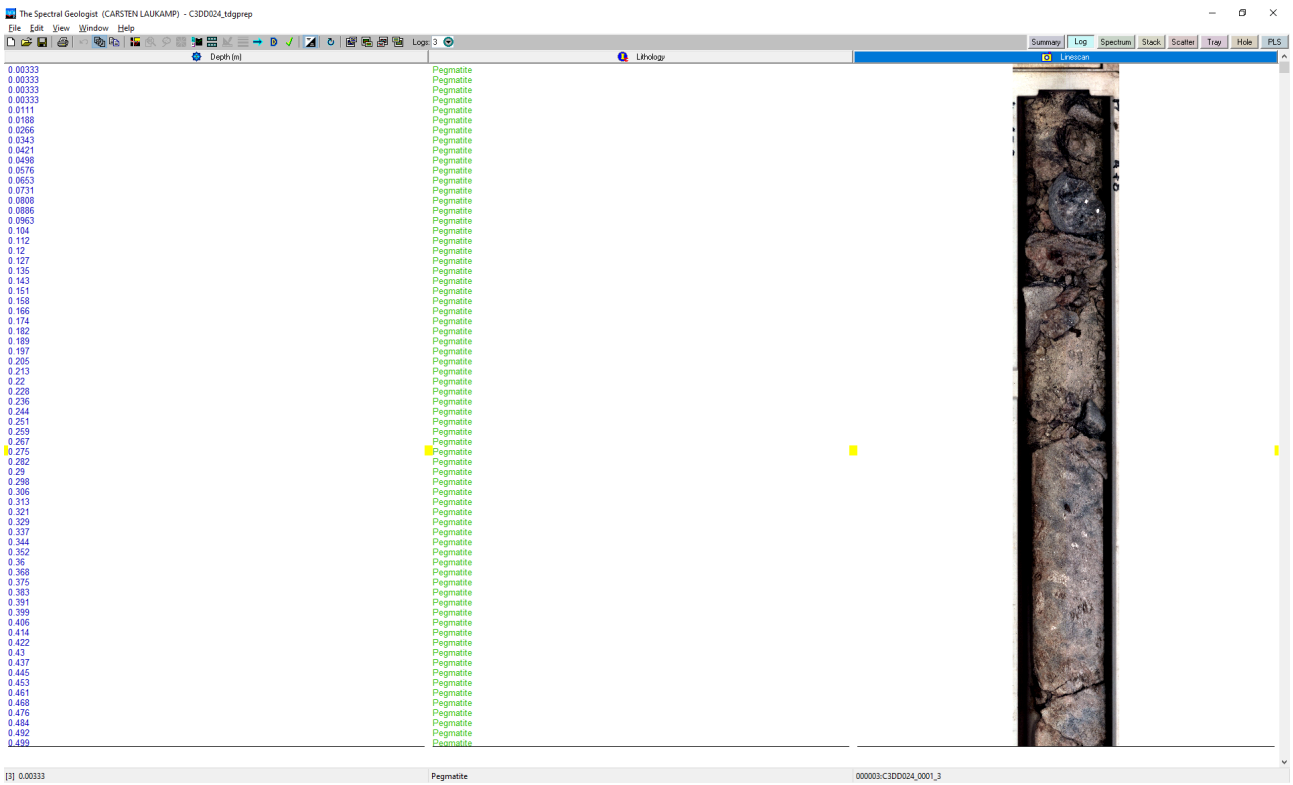


**Figure 9 Plot layout "log lithology"**

## 1.4 Plot layout "scatter spodumene"

This plot layout shows VNIR-SWIR reflectance spectra (top left) and TIR reflectance spectra (middle left) as well as the following scatter plots:

- top right: depth (x-axis), XRF-derived $Li_2O$ (y-axis), coloured by the relative intensity of a trough at around 11500 nm diagnostic for spodumene (11500D)
- middle right: depth (x-axis), relative intensity of a trough at around 11500 nm diagnostic for spodumene (11500D) (y-axis), coloured by the XRF-derived $Li_2O$
- bottom right: depth (x-axis), Aux-match of spodumene reference sample M2082 (y-axis), coloured by the relative intensity of a trough at around 11500 nm diagnostic for spodumene (11500D)
- bottom left: XRF-derived $Li_2O$ (x-axis), relative intensity of a trough at around 11500 nm diagnostic for spodumene (11500D) (y-axis), coloured by the system-based jCLS TIR results of the first mineral group identified in the TIR

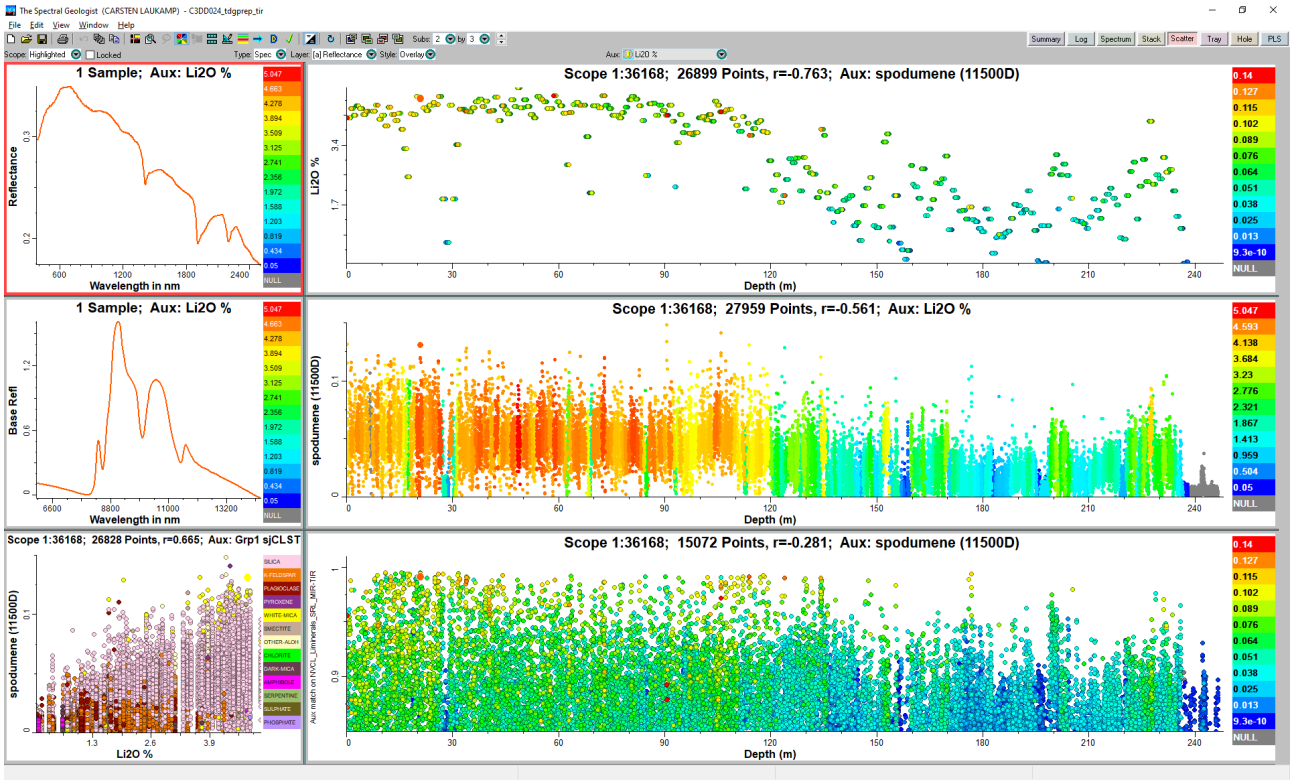


Figure 10 Plot layout “scatter spodumene”

## 1.5 Plot layout “log PLS”

This plot layout features from left to right the depth (1st column), three pairs of XRF-derived and PLS-modelled geochemical parameters ($K_2O$, $Li_2O$, $SiO_2$, $K_2O+Na_2O/SiO_2$) in columns 2 to 9, selection of calibration (C) and test (T) samples used for the PLS-based prediction of the respective geochemical parameters (column 10) and the relative intensity of a trough at around 11500 nm diagnostic for spodumene (11500D) (column 11).

Figure 11 Plot layout “log PLS”

## 1.6 Plot layout “scatter PLS K”

This plot layout comprises scatter plots:

- Top left: XRF-derived $SiO_2$ (x-axis), XRF-derived $K_2O$ (y-axis), coloured by XRF-derived $Li_2O$
- Top right: depth (x-axis), XRF-derived $K_2O$ (y-axis), selection of calibration (C ) and test (T) samples used for the PLS-based prediction of the respective geochemical parameters
- Middle left: XRF-derived $K_2O$ (x-axis), PLS-based modelling of $K_2O$ using only the 50 to 250 m depth interval (y-axis), coloured by the system-based jCLS TIR results of the first mineral group identified in the TIR
- Middle right: depth (x-axis), PLS-based modelling of $K_2O$ using only the 50 to 250 m depth interval (y-axis), coloured by XRF-derived $K_2O$
- Bottom left: TIR reflectance spectra
- Bottom right: depth (x-axis), XRF-derived $K_2O$ (y-axis), coloured by PLS-based modelling of $K_2O$ using only the 50 to 250 m depth interval

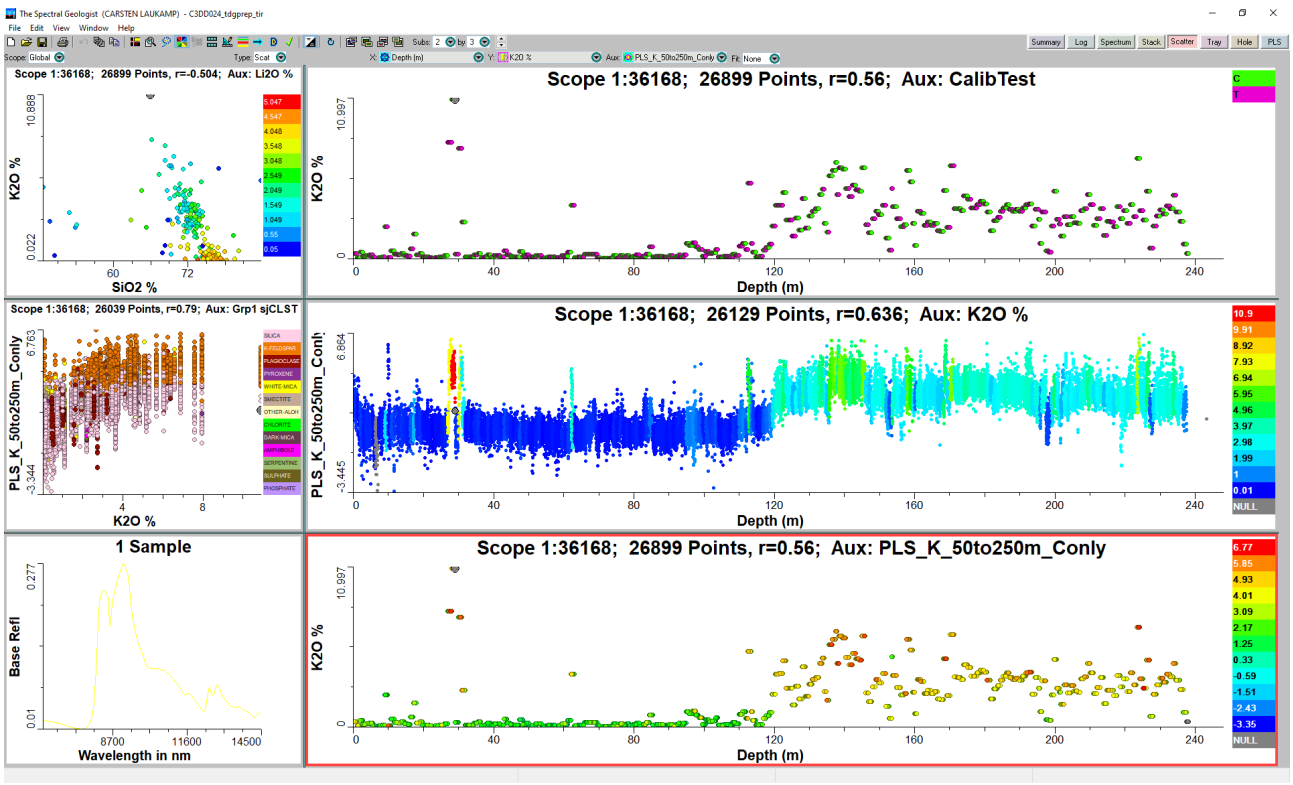


Figure 12 Plot layout “scatter PLS K”

## 1.7 Plot layout “scatter PLS KNaSi”

This plot layout comprises scatter plots:

- Top left: XRF-derived $LiO_2$ (x-axis), $K_2O+Na_2O/SiO_2$ (y-axis), coloured by XRF-derived $Li_2O$
- Top right: depth (x-axis), $K_2O+Na_2O/SiO_2$ (y-axis), selection of calibration (C ) and test (T) samples used for the PLS-based prediction of the respective geochemical parameters
- Middle left: $K_2O+Na_2O/SiO_2$ (x-axis), PLS-based modelling of $K_2O+Na_2O/SiO_2$ (y-axis), coloured by the system-based jCLS TIR results of the first mineral group identified in the TIR
- Middle right: depth (x-axis), PLS-based modelling of $K_2O+Na_2O/SiO_2$ (y-axis), coloured by $K_2O+Na_2O/SiO_2$
- Bottom left: TIR reflectance spectra
- Bottom right: depth (x-axis), $K_2O+Na_2O/SiO_2$ (y-axis), coloured by PLS-based modelling of $K_2O+Na_2O/SiO_2$

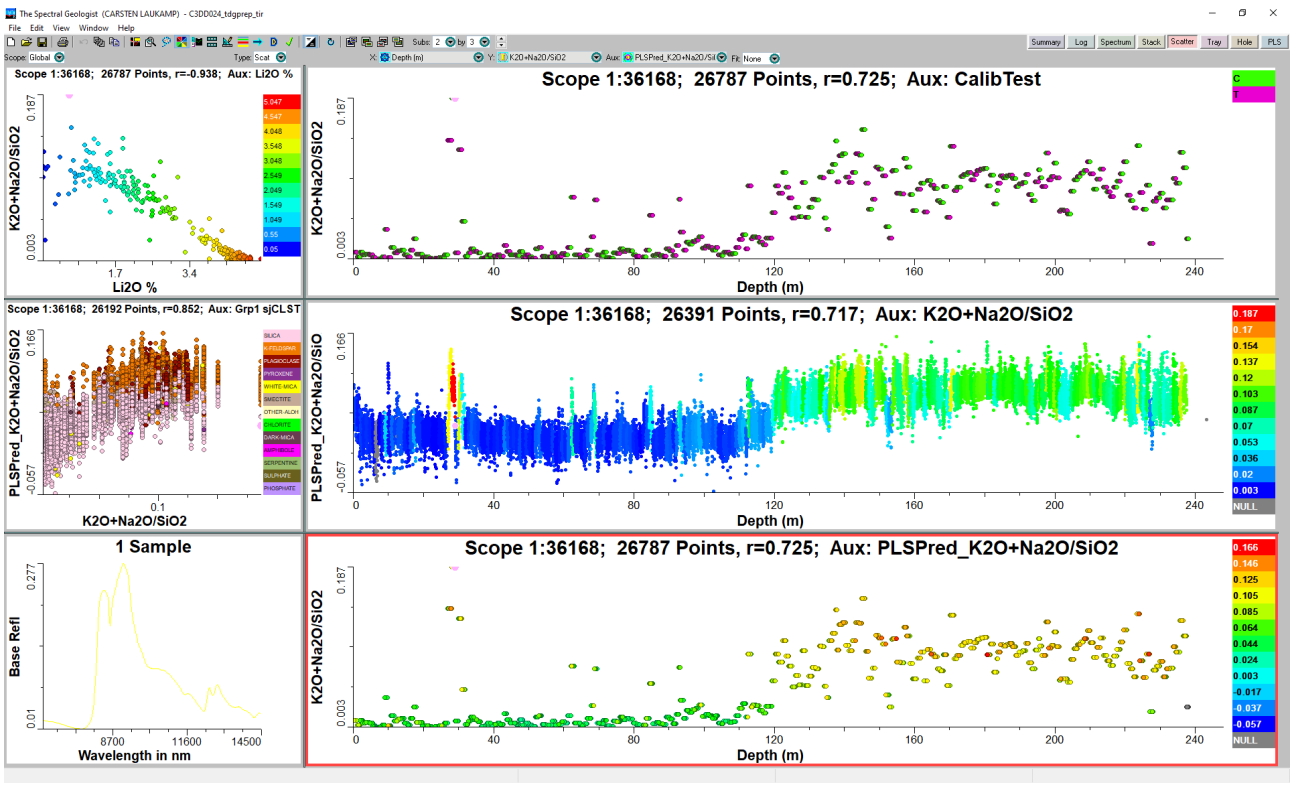


Figure 13 Plot layout “scatter PLS KNaSi”

## 1.8 Plot layout “tray8 KNaSi PLS”

This plot layout shows the high resolution RGB imagery of tray 8. The top colour ribbon of each section shows $K_2O+Na_2O/SiO_2$ calculated from XRF results. The bottom colour ribbon shows the PLS-based $K_2O+Na_2O/SiO_2$.

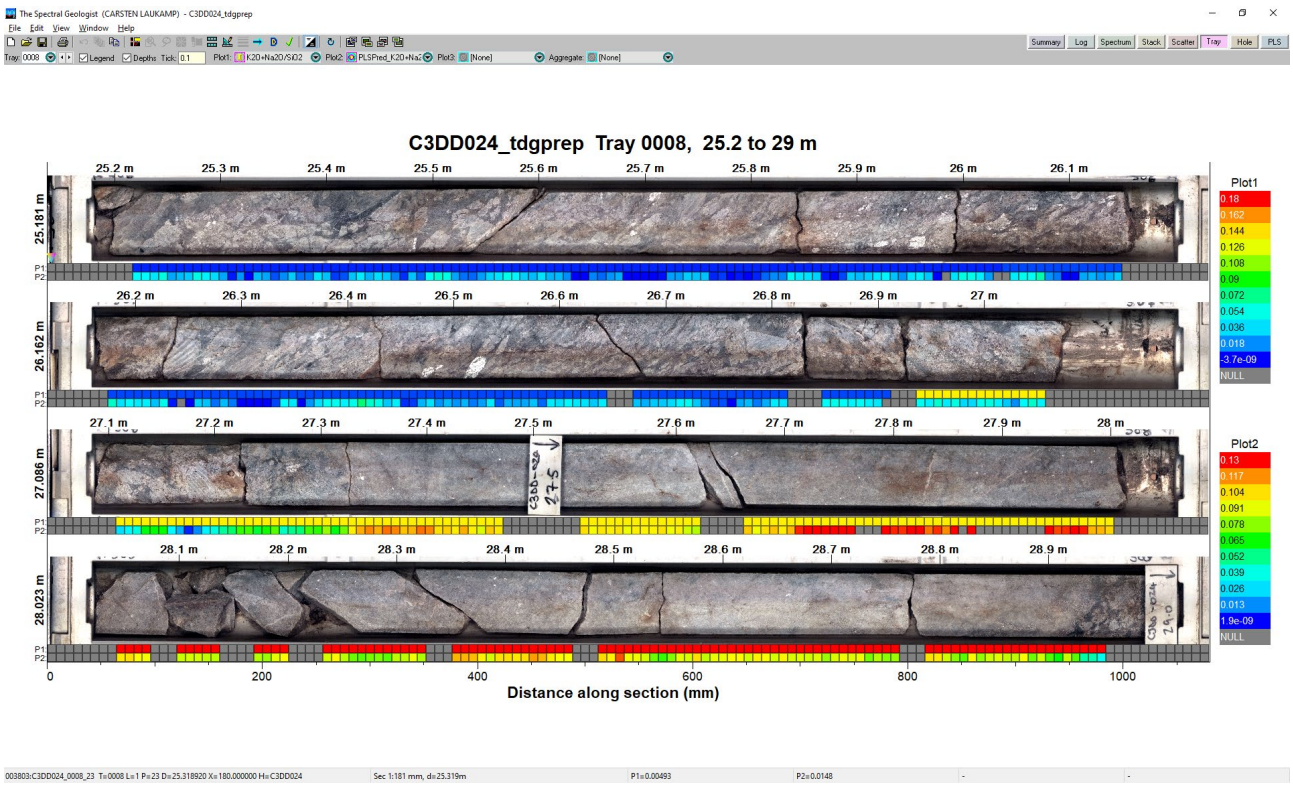


Figure 14 Plot layout “tray8 KNaSi PLS”

# Acknowledgments

The National Virtual Core Library is supported by AuScope (www.auscope.org), the Australian Government National Collaborative Research Infrastructure Strategy (NCRIS), the CSIRO and Australian state and territory geological surveys. We would like to express our sincere thanks to those who successfully initiated the NVCL over 10 years ago and helped to build a strong infrastructure that new generations can build upon. First and foremost, we thank Jon Huntington (former NVCL Director) and Lew Whitbourn (former Hyperspectral Engineering Team Leader) who made the NVCL with their teams possible.

Furthermore, we’d like to acknowledge all those hard-working people that collect and process the NVCL data on a day to day basis, helping to ‘uncover the mineralogy of the top two kilometres of the Australian continent’, and particular, the HyLogging team at the Geological Survey of Western Australia for creating this dataset.

# References


Berman, M., Bischof, L., Lagerstrom, R., Guo, Y., Hungtington, J., Mason, P., Green, A. (2017) A comparison between three sparse unmixing algroithms using a large library of shortwave infrared mineral spectra.- IEEE Transactions on Geoscience and Remote Sensing, 55 (6), 3588-3610.

Hancock, EA, Green, AA, Huntington, JF, Schodlok, MC and Whitbourn, LB 2013, HyLogger-3: Implications of adding thermal-infrared sensing: Geological Survey of Western Australia, Record 2013/3, 24p.

Hancock, EA and Huntington, JF 2010, The GSWA NVCL HyLogger: rapid mineralogical analysis for characterizing mineral and petroleum core: Geological Survey of Western Australia, Record 2010/17, 21p.

Hancock, EA and Wawryk, M 2020, Drillhole C3DD024: Hyperspectral logging of diamond core; HyLogger record 2020/21: Geological Survey of Western Australia, 10p.

Laukamp, C., Cudahy, T., Caccetta, M., Chia, J., Gessner, K., Haest, M., Liu, Y.C., Rodger, A. (2010): The uses, abuses and opportunities for hyperspectral technologies and derived geoscience information.- AIG Bulletin, 51 (Geo-Computing 2010 Conference, Brisbane, September 2010): 73-76.

Laukamp, C., Stromberg, J., Francis, N., Mule, S., LeGras, M., Hauser, J. (2020): Examples of integrating hyperspectral, geochemical and petrophysical data - NVCL data integration report FY20 - CSIRO report EP207514.

Laukamp, C., Rodger, A., LeGras, M., Lampinen, H., Lau, I., Pejcic, B., Stromberg, J., Francis, N., Ramanaidou, E. (2021): Mineral physicochemistry underlying feature-based extraction of mineral abundance and composition from shortwave, mid and thermal infrared reflectance spectra. Minerals, 11(4), 347

Partington, G.A., McNaughton, N.J. and Williams, I.S., 1995. A review of the geology, mineralization, and geochronology of the Greenbushes pegmatite, Western Australia. *Economic Geology*, *90*(3), pp.616-635.

Partington, G.A., 1990. Environment and structural controls on the intrusion of the giant rare metal Greenbushes pegmatite, Western Australia. *Economic Geology*, *85*(3), pp.437-456.

Partington, G.A., 2017. Greenbushes tin, tantalum and lithium deposit, in *Australian Ore Deposits* (ed: G N Phillips), pp 153-157 (The Australasian Institute of Mining and Metallurgy: Melbourne)

Schodlok, MC, Whitbourn, L, Huntington, J, Mason, P, Green, A, Berman, M, Coward, D, Connor, P, Wright, W, Jolivet, M and Martinez, R 2016, HyLogger-3, a visible to shortwave and thermal infrared reflectance spectrometer system for drill core logging: functional description: AJES, v. 63, no. 8, p. 929–940.

Sweetapple, M.T., 2017. A review of the setting and internal characteristics of lithium pegmatite systems of the Archaean North Pilbara and Yilgarn Cratons, Western Australia. In *Granites 2017 Conference Benalla Victoria, Ext Abstr Austr Inst Geosci Bull* (Vol. 65).

GSWA WAMEX Report A0104943

https://www.talisonlithium.com/greenbushes-project

# Additional Resources

**AuScope Discovery Portal**
http://portal.auscope.org/

**Instructional Videos**

"How to download TSG Files from the Auscope Discover Portal"
https://www.youtube.com/watch?v=Oh_YAxEpLeo&t=115s

"Introduction to working with HyLogger Data in The Spectral Geologist (TSG)"
https://www.youtube.com/watch?v=u-SjA2_J3RQ&t=71s

**Recorded Webinars**

"The National Virtual Core Library – Building a Continental-Scale drill core database"
https://www.youtube.com/watch?v=AlcIqAGc9U4&t=4s

"Mineral composition trends in hydrothermal mineral systems inferred from reflectance spectra"
https://www.youtube.com/watch?v=IEvxn6o0imk&t=110s

**Other TSG Materials**
https://research.csiro.au/thespectralgeologist/support/downloads/

**CSIRO Spectral Reference Library**
http://mineralspectrallibraries.csiro.au/

**As Australia's national science agency and innovation catalyst, CSIRO is solving the greatest challenges through innovative science and technology.**

CSIRO. Unlocking a better future for everyone.

**For further information**

M**ineral Resources**
Dr. Jessica Stromberg
Jessica.stromberg@csiro.au